Journal of the Optical Society of America A
OPTICS, IMAGE SCIENCE, AND VISION

Enhancement of Rayleigh scattering in a two-dimensional Fabry–Perot resonator loaded with impurities

ALMAS F. SADREEV

Kirensky Institute of Physics, Siberian Branch of Russian Academy of Sciences, 660036 Krasnoyarsk, Russia (almas@tnp.krasn.ru)

Received 11 February 2016; revised 15 May 2016; accepted 17 May 2016; posted 19 May 2016 (Doc. ID 259273); published 8 June 2016

We study wave transmission through a Fabry–Perot resonator (FPR) loaded with point-like impurities. We show both analytically in the framework of the coupled mode theory and numerically that there are two different regimes for transmission dependent on the quality of the FPR mirrors. For low quality, we obtain transmittance very similar to the clean FPR with slightly shifted Lorentz peaks. However, for good quality, the transmittance peaks are strongly reduced and substituted with Gaussian peaks because of multiple scattering of waves by each impurity. As a side effect, we observe the angular (channel) conversion in the disordered FPR. We demonstrate that the resonant peaks are dependent on the concentration of impurities to pave a way for resonant measurement of the concentration.

OCIS codes: (050.2230) Fabry-Perot; (290.4210) Multiple scattering; (290.3700) Linewidth; (290.5870) Scattering, Rayleigh.

http://dx.doi.org/10.1364/JOSAA.33.001277

1. INTRODUCTION

The study of wave scattering by small particles has had a long history since the work by Rayleigh [1]. Wave transmission through opaque media is still a subject of interest in daily life; see, for example, reviews [2,3] and the book by Ishimaru [4]. The problem of multiple scattering by random media composed of many discrete particles is an important subject of research owing to the wide range of possible applications in academic research and industry. Over the past few decades, the multiple scattering of plane waves by random discrete particles has been extensively investigated. Many methodologies have been developed to analyze this problem, for instance, multiple scattering theory [2,3,5], the T-matrix method [6–10], and many hybrid numerical methods (see, for example, Ref. [9]). The basic result of such multiple scattering is that the wave nature of light leads to a reduction in transmittance due to destructive interference effects [10–13].

We consider the resonant transmission through a Fabry–Perot resonator (FPR) filled with isotropic point-like impurities in the weak disorder regime. The presence of FPR mirrors leads to the enhancement of Rayleigh scattering due to multiple reflections from the mirrors. In other words, the effective length of disordered sample L can be considerably enlarged in the FPR. The effective length depends on the quality factor of the mirrors given by the inverse of the resonance width $1/\Gamma$. The measure of disorder within the FPR cell defined by the concentration of impurities can be specified by the inhomogeneous line width γ. In order to preserve the resonant transmission, we imply that $\Delta\omega \gg \gamma, \Gamma$, where $\Delta\omega$ is the distance between the nearest resonant peaks of the FPR. The aim of the present paper is to show that the resonant transmission strongly depends on the ratio γ/Γ. If $\gamma \ll \Gamma$, we obtain Lorentz resonant peaks slightly shifted by mean values of the dielectric constant of impurities. However, if $\gamma \gg \Gamma$, the Lorentz resonant peaks are substituted with Gaussian-shaped peaks with the height substantially reduced by the factor Γ/γ.

We obtain these results analytically in the framework of the coupled mode theory (CMT) and show that they are in a good agreement with the numerical results. Although the present consideration is simple, it establishes two features which have important applications. The first result shows that the concentration of impurities can be measured by the positions of resonant peaks. The second result is the channel conversion for light transmission through the loaded FPR that also gives additional information about the impurities.

2. EFFECTIVE HAMILTONIAN APPROACH

In what follows, we restrict ourselves to a two-dimensional FPR formed by two identical dielectric slabs with high dielectric constant ε_0. The inner space between the slabs is filled with impurities with dielectric constant ε, as shown in Fig. 1. That restriction can be justified if we present each impurity as a dielectric rod directed along the z-axis packed randomly between the slabs. The case of a single rod in the FPR was considered in

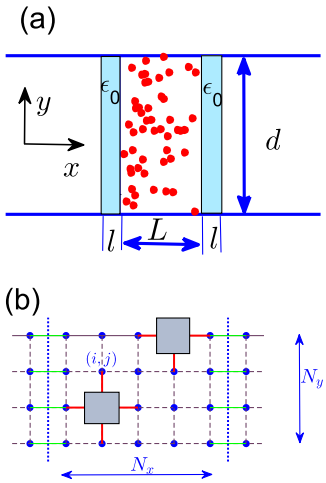

Fig. 1. (a),(b) FPR resonator formed by two dielectric slabs with high dielectric constant ε and filled with point-like impurities with the dielectric constant ε.

Ref. [14]. Then if, for example, the TM mode with wave vector $\mathbf{k} = (k_x, k_y)$ is injected from the left, the impurities scatter into different directions. However, there are no processes of scattering into the TE modes. Therefore, we can write the Maxwell equations in the scalar form as

$$\nabla \frac{1}{\varepsilon(x,y)} \nabla \psi(x,y) + \omega^2 \psi(x,y) = 0, \tag{1}$$

where $\psi = E_z$ is the electric field directed along the z-axis, and the dielectric constant $\varepsilon(x,y)$ is unity everywhere except at the impurities. The FPR is remarkable in that for any fixed frequency $\omega^2 = k_x^2 + k_y^2$, light transmits at a discrete sequence of the incident angles [15]

$$\cos \alpha_n = \frac{\pi n}{kL}, \qquad n = 0, \pm 1, \pm 2, \ldots, \tag{2}$$

where L is the width of the FPR cell. Preservation of $k_y = \omega \sin \alpha$ implies that there are no transitions between angles α_n, which is a result of space homogeneity across the transport axis normal to the mirror's plane. In what follows, the light velocity is taken as unity. We take that the inner space of the clean FPR has a unity dielectric constant.

In practice, the sizes of the slabs or mirrors along the y-axis are restricted. Therefore, we confine the space along the transverse axis $y \in [0d]$, imposing the Dirichlet boundary conditions. Then from Eq. (1), we obtain

$$\omega^2 = \left[k_p^2 + \frac{\pi^2 p^2}{d^2} \right], \tag{3}$$

where $p = 1, 2, 3, \ldots$ enumerates propagating channels in the waveguide and d is the width of the waveguide as shown in Fig. 1. The propagating states in the waveguide are the following:

$$\psi_p(x,y) = \sqrt{\frac{1}{\pi d k_p}} \sin \frac{\pi p y}{d} e^{i k_p x}. \tag{4}$$

The implications of dielectric slabs or one-dimensional photonic crystal mirrors [14] split the system into five parts: the left and right waveguides, two dielectric slabs shown in blue in Fig. 1 and the inner space between the slabs with size $L \times d$, and the FPR cell, filled by impurities. Each slab preserves the channel number p, or, in other words, does not mix the channels. The dielectric slabs suppress the transmittance which can be expressed via the transfer matrix [16] for each channel p,

$$M_{11}^{(p)} = \cos(q_p a) + \frac{i}{2}\left[\frac{q_p}{k_p} + \frac{k_p}{q_p}\right] \sin(q_p l),$$

$$M_{12}^{(p)} = \frac{i}{2}\left[\frac{q_p}{k_p} - \frac{k_p}{q_p}\right] \sin(q_p l),$$

$$M_{22}^{(p)} = (M_{11}^{(p)})^*, \qquad M_{21}^{(p)} = (M_{12}^{(p)})^*,$$

$$t_p = \frac{1}{M_{22}^{(p)}}, \qquad r_p = \frac{M_{12}^{(p)}}{M_{22}^{(p)}}, \tag{5}$$

where k_p is given by Eq. (3), and

$$q_p^2 = \varepsilon k_p^2 + (\varepsilon - 1)\pi^2 p^2. \tag{6}$$

If the FPR cell were clean, the total transmittance would have the form [15]

$$T_p = \frac{t_p^2 e^{ikL}}{1 - r_p^2 e^{2ikL}}. \tag{7}$$

The transmittance in the first channel $p = 1$ described by Eq. (7) is shown in Fig. 2 by a solid line.

The situation changes if the FPR cell is filled by the impurities because of conversion between different channels p. Then Eq. (7) shall be substituted by the following equation:

$$\widetilde{T}_{pp'} = t_p T_{pp'} t_{p'}, \tag{8}$$

where calculation of the transmittance $T_{pp'}(\omega)$ through the FPR cell filled by randomly distributed impurities is the main subject of our consideration below. The single impurity in the form of a dielectric cylinder between the delta-like slabs admits analytical consideration [14]. The case of many impurities can be considered numerically or by perturbation theory for weak Rayleigh scattering when the size of the impurities is substantially less than the wavelength.

Our approach for the calculation of light transmittance through the FPR cell with impurities is based on the Feshbach projection of the total Hilbert space of the full Hamiltonian

$$\widehat{H} = \widehat{H}_c + \widehat{V} + \widehat{H}_L + \widehat{H}_R + \widehat{W}_L + \widehat{W}_R \tag{9}$$

into the inner space of the FPR cell [17,18]. Here, $\widehat{H}_c$ is the Hamiltonian of the closed clean FPR cell, $\widehat{H}_L, \widehat{H}_R$ are the

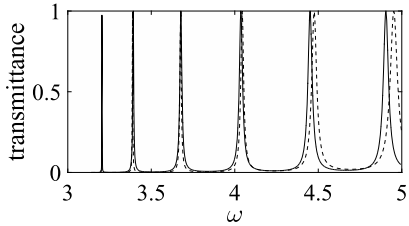

Fig. 2. Transmittance through the clean FPR in the first channel. The dashed line shows the transmittance in the FPR with $\varepsilon_0 = 10$, $a = 1/10$, and $L = 5$. The solid line shows the tight-binding approach in Eq. (26) with $v = 0.75$, $N_x = 100$, and $N_y = 20$.

Hamiltonians of left and right waveguides with the continua of eigenmodes from Eq. (4), respectively, $\widehat{W}_L = \widehat{W}_R$ are the coupling matrices between the FPR cell and the waveguides, and $\widehat{V}$ is the Hamiltonian of the impurities whose explicit form will be given below. That procedure defines an effective non-Hermitian Hamiltonian as follows [17,18,19–21]:

$$\widehat{H}_{\text{eff}} = \widehat{H}_c + \widehat{V} + \widehat{W}\frac{1}{\widehat{H}_W - \omega^2 - i0}\widehat{W}^+. \tag{10}$$

Then the solution for the scattering state ψ projected onto the FPR cell is given by the Lippmann–Schwinger equation [22–24] as

$$(\widehat{H}_{\text{eff}} - \omega^2)\psi = i\widehat{W}_L\psi_{\text{in}}, \tag{11}$$

where ψ_{in} is the wave injected via the left waveguide. Respectively, the scattering matrix consisted of transmission and reflection amplitudes $T_{pp'}$ and $R_{pp'}$ defined by the Green function of Eq. (11) [20,21]:

$$\widehat{S} = 2\widehat{W}^+\frac{1}{\widehat{H}_{\text{eff}} - \omega^2 + i0}\widehat{W}. \tag{12}$$

The effective Hamiltonian acquires the Wigner–Weisskopf form in the approximation of the infinite band of waveguides [17,18,19–21]

$$\widehat{H}_{\text{eff}} = \widehat{H}_c + \widehat{V} - i\widehat{W}\widehat{W}^+, \tag{13}$$

where $\widehat{H}_c$ is the diagonal matrix of the eigenfrequencies of Eq. (25), $\widehat{W}$ is the coupling matrix [21,22,25]

$$W_{mn,p} = \sqrt{\frac{1}{\pi k_p}}\int_0^d \mathrm{d}y\psi_p(x,y)\frac{\partial\psi_{mn}(x,y)}{\partial x}\bigg|_{x=x_b}, \tag{14}$$

where integers m and n enumerate the eigenmodes of the clean FPR cell

$$\psi_{mn}(x,y) = \frac{2}{\sqrt{Ld}}\sin\frac{\pi m x}{L}\sin\frac{\pi n y}{d}, \tag{15}$$

with the eigenfrequencies

$$\omega_{mn}^2 = \pi^2 c^2\left(\frac{m^2}{L^2} + \frac{n^2}{d^2}\right). \tag{16}$$

Substitution of the eigenmodes from Eqs. (4) and (24) into Eq. (14) immediately gives us

$$W_{mn,p} = W_{m,p}\delta_{np} = \sqrt{\frac{2}{\pi k_p L}}k_m\delta_{np}, \tag{17}$$

where $1/k_p$ and L are measured in the waveguide width d. Therefore, for the clean FPR, the S-matrix is diagonal over channel p with typical resonant transmittance, as shown in Fig. 2.

As was mentioned above, we consider impurities as rods with the dielectric constant ε. That defines the perturbation matrix elements $\widehat{V}$ in the space of the eigenmodes from Eq. (24) as follows according to the Maxwell equation [Eq. (1)]:

$$V_{mn,m'n'} = \left(1 - \frac{1}{\varepsilon}\right)\sum_{j=1}^{N_i}\int \mathrm{d}^2\mathbf{x}\nabla\psi_{mn}(\mathbf{x} - \mathbf{x}_j)\nabla\psi_{m'n'}(\mathbf{x} - \mathbf{x}_j), \tag{18}$$

where integration is performed within each impurity. According to Eqs. (8), (12), and (18), the transmittance will take the following form:

$$\widetilde{T}_{pp'}(\omega) = \sum_{mm'}\frac{2W_{m,p}W_{m',p'}}{E_{mp}\delta_{mm'}\delta_{pp'} + V_{mp,m'p'} - \omega^2 - i2W_{mp}W_{m'p'}}, \tag{19}$$

where the factor 2 is a result of two identical waveguides: left and right.

3. NUMERICAL SIMULATIONS

Direct computation of light transmittance through the FPR cell filled by impurities by use of Eq. (19) is numerically time consuming, because it involves evaluation of the inverse of the nonsparse matrix $\widehat{H}_{\text{eff}} - \omega^2$. In practice, to speed up the performance, one can use the finite difference methods or truncate the effective Hamiltonian. In this section, we present numerical results based on the first approach. Using standard discretization of the derivatives [26], we have

$$\frac{\partial}{\partial x}\xi(x)\frac{\partial}{\partial x}\psi(x) = \frac{1}{a_0^2}[\xi_{i+1/2}(\psi_{i+1} - \psi_i) - \xi_{i-1/2}(\psi_i - \psi_{i-1/2})], \tag{20}$$

where $\xi(x,y) = \frac{1}{\varepsilon(x,y)}$. We obtain the following tight-binding approximation of wave Eq. (1):

$$t_{ij}(\psi_{i+1,j} + \psi_{i-1,j} + \psi_{i,j+1} + \psi_{i,j-1}) - \lambda_{i,j}\psi_{i,j} = a_0^2\omega^2\psi_{i,j}, \tag{21}$$

$$t_{ij} = \begin{cases} 1/\varepsilon, & \text{if an impurity occupies site } i,j; \\ 1, & \text{otherwise,} \end{cases} \tag{22}$$

$$\lambda_{ij} = \begin{cases} 4/\varepsilon, & \text{if an impurity occupies site } i,j; \\ 4, & \text{otherwise.} \end{cases} \tag{23}$$

That model of dielectric impurities corresponds to the Anderson model with both diagonal and off-diagonal disorders [27]. In the tight-binding representation of the Hamiltonian [22], we have

$$\psi_{mn}(i,j) = \frac{2}{\sqrt{(N_x+1)(N_y+1)}}\sin\frac{\pi m i}{N_x+1}\sin\frac{\pi n j}{Ny+1}, \tag{24}$$

with the eigenfrequencies

$$\omega_{mn}^2 = N_y^2\left[4 - 2\cos\left(\frac{\pi m}{N_x}\right) - 2\cos\left(\frac{\pi n}{N_y}\right)\right]. \tag{25}$$

The effective Hamiltonian modifies [22,24,28] as follows:

$$\widehat{H}_{\text{eff}} = \widehat{H}_c + \widehat{V} - v^2\sum_p \phi_p\exp(ik_p a_0)\phi_p^+(\delta_{j,1} + \delta_{j,N_x}), \tag{26}$$

where $\phi_p(j) = \sqrt{\frac{2}{N_y+1}}\sin(\frac{k_p j}{N_y+1})$ are discretized transverse solutions, and v is the hopping matrix element between the waveguides and the FPR cell depicted by solid green lines in Fig. 1(b). The parameter $v < 1$ controls the quality of the

FPR mirrors and defines the resonant widths $\Gamma \sim v^2$ [22,29]. The effective Hamiltonian in Eq. (26) coincides with the Hamiltonian of the FPR cell everywhere except at the boundaries $j_x = 1, N$. Comparison of the present tight-binding approach for $v = 0.75$ with the exact continual approach in Eq. (7) for the clean FPR demonstrates good agreement that justifies the simulation of the FPR mirrors in the form of dielectric slabs by the hopping matrix element $v < 1$. This approximation is equivalent to $t_p(\omega)$ being independent of the frequency in Eq. (8).

The computational results are presented in Fig. 3 for high-quality FPR mirrors. In Figs. 3(a) and 3(b), one can see the following effects associated with the growth of the impurity concentration $c = N_i/N$, where N_i is the number of impurities, and $N = N_x N_y$. (i) For small concentration c, the positions of the Lorentz peaks are slightly shifted by a distance proportional to the concentration, as shown in Figs. 3(a) and 3(b) by closed circles. That is a trivial consequence of a small change in the mean dielectric constant due to the impurities. (ii) A further increase in the impurities concentration causes a substantial suppression of resonant peaks and an increase in resonant widths, as shown by open circles in Figs. 3(a) and 3(b). Figure 3(c) demonstrates the weak effect of channel conversion due to Rayleigh scattering by the impurities. Because of the FPR mirrors, the conversion also shows resonant behavior versus the impurities concentration c. (iii) Figure 3(d) shows that the impurities concentration c can serve as a control parameter which affects resonant peaks similar to the incident angle in Eq. (2) or frequency. This result was used to tune the resonant modes of a FPR cell filled with gold nanoparticles [30]. It is remarkable that for small c one can observe a Lorentz resonant peak, while for larger c the peak is close to the Gaussian form with reduced height. The above results will be reproduced analytically in the next section in the framework of the CMT theory.

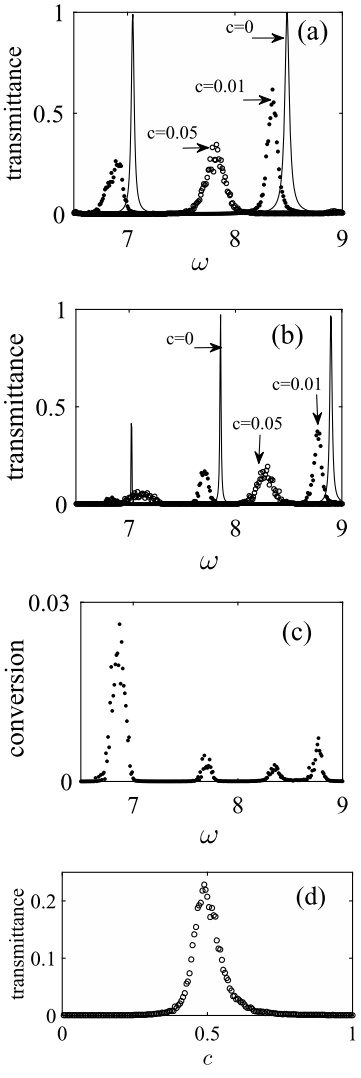

Fig. 3. Average over impurities positions transmittance versus frequency for $c = 0$ (solid line), $c = 0.05$ (closed circles), and $c = 0.2$ (open circles) in (a) the first channel $p = 1$ and (b) the second channel. (c) Transmittance between channels (conversion) for $c = 0.2$. (d) Transmittance versus impurities concentration for $\omega = 7$. The parameters of the numerical simulations are $v = 0.5, \varepsilon = 1.25$, $N_x = 60$, and $N_y = 30$. The frequency is measured in terms of light velocity/width of the waveguide.

4. COUPLED MODE THEORY

The Lippmann–Schwinger equation [Eq. (11)] can be written in the basis of the eigenmodes of the closed clean FPR resonator Eq. (24) enumerated by the indices m, n. Expanding the scattering function within the FPR cell over the eigenmodes $\psi(x, y) = \Sigma_{mn} A_{mn} \psi_{mn}(x, y)$, we obtain from Eq. (11) with account of Eq. (17)

$$(\omega_{mp}^2 - \omega^2) A_{mp} - 2i \sum_{m'} \sqrt{\Gamma_{mp} \Gamma_{m'p}}\, A_{m'p} = i \sqrt{\Gamma_{mp}} E_0 - \sum_{m'p'} V_{mp,m'p'} A_{m'p'}, \quad (27)$$

where $\Gamma_{mp} = W_{mp}^2$, and the EM wave with amplitude E_0 is injected in the channel $p = n$. For the clean FPR $V_{mp,m'p'} = 0$, Eq. (27) is the stationary coupled mode equation derived in Refs. [31,32]. Thus, the Lippmann–Schwinger Eq. (11) with the effective non-Hermitian Hamiltonian in the Wigner–Weiskopf form is equivalent to the CMT [23,24]. As seen from Eq. (27), any inclusions within the FPR cell give rise to channel conversion $p \to p'$ [14].

For a high quality factor of the FPR mirrors $\Gamma_a \ll |\omega_{mp} - \omega_{m'p}|$ and a small effect of the impurities $|V_{mn,m'n'}| \ll |\omega_{mp} - \omega_{m'p}|$, we can restrict ourselves by single eigenmode approximation in the CMT Eq. (27). We show that all features of wave transmission through the loaded FPR except the channel conversion can be described by this approximation. Let ψ_a be the eigenmode of the closed FPR cell with $\omega \approx \omega_a$, where for brevity we introduced $a = (m, p)$. As shown in the previous section, in the clean FPR the eigenmode a is coupled only with scattering channel $p = n$. Then the CMT Eq. (27) will take the most simple form of

$$(\omega^2 - \omega_a^2 - V_{aa} + 2i\Gamma_a) A_a = -i \sqrt{\Gamma_a} E_0, \quad (28)$$

where E_0 is the amplitude of the incident monochromatic light. Before averaging over the positions of impurities, the transmittance amplitudes have Breit–Wigner form

$$T_{pp}^{(1)}(\omega) = \frac{2\Gamma_a}{\omega^2 - \omega_a^2 - V_{aa} + i2\Gamma_a}. \quad (29)$$

Here, the superscript "(1)" denotes the first order of the perturbation theory. In accordance with Eqs. (17) and (21), we can establish a correspondence between the former tight-binding approach and the present CMT decay parameters as

$$\Gamma_a = \Gamma_{mp} = \frac{2v^2}{\pi k_p L}. \quad (30)$$

Assume that the impurities are uncorrelated and distributed randomly inside the FPR cavity. Then the probability distribution of matrix elements in Eq. (18) can be easily evaluated by use of a central limit theorem that gives

$$\begin{aligned}\rho(V_{ab}) &= \left\langle \delta(V_{ab} - (1-1/\varepsilon)\sum_{j=1}^{N} \nabla\psi_a(\mathbf{x}_j)\nabla\psi_b(\mathbf{x}_j)\right\rangle \\ &= \frac{1}{2\pi}\int_{-\infty}^{\infty} d\mu e^{i\mu(V_{ab} - Na_0^2(1-1/\varepsilon))} \\ &\quad \times \left\{\int d^2\mathbf{x} e^{i\mu(1-1/\varepsilon)a_0^2\nabla\psi_a(\mathbf{x})\nabla\psi_b(\mathbf{x})}\right\}^N \\ &\approx \frac{1}{2\pi} e^{Nf(0)}\int_{-\infty}^{\infty} d\mu \exp\left\{i\mu V_{ab} - \frac{N}{2}f''(0)\mu^2\right\} \\ &= \frac{1}{\sqrt{2\pi\sigma_{ab}}}\exp[-(V_{ab} - \langle V_{ab}\rangle)^2/2\sigma_{ab}^2], \end{aligned} \quad (31)$$

where

$$f(\mu) = \ln\int d^2\mathbf{x}\exp[-i\mu(1-1/\varepsilon)a_0^2\nabla\psi_a(\mathbf{x})\nabla\psi_b(\mathbf{x})],$$

$$f''(0) = (1-1/\varepsilon)^2 a_0^4[\langle\nabla\psi_a\nabla\psi_b\rangle^2 - \langle(\nabla\psi_a)^2(\nabla\psi_b)^2\rangle],$$

and

$$\sigma_{ab} = \langle(V_{ab} - \langle V_{ab}\rangle)^2\rangle, \sigma_{aa} = \sigma_{bb} = \sigma_{ab}/2 \approx (1-1/\varepsilon)^2 c. \quad (32)$$

Here, $\langle\cdots\rangle$ means average over positions of the impurities, i.e., integration over $\mathbf{x} = (x, y)$. Asymptotical evaluation of the average over the distributions in Eq. (31) gives us the following expressions for averaged transmittance:

$$\begin{aligned}\langle|T_{pp}^{(1)}(\omega)|^2\rangle &= \int |T_{pp}^{(1)}|^2\rho(V_{aa})dV_{aa} \\ &\approx \begin{cases} \frac{\Gamma_a^2}{(\omega^2 - \omega_a^2 - \langle V_{aa}\rangle)^2 + \Gamma_a^2}, & \text{if } \sigma_{aa} \ll \Gamma_a \\ \frac{\Gamma_a}{\sigma_{aa}}\exp\left[-\frac{(\omega^2 - \omega_a^2 - \langle V_{aa}\rangle)^2}{2\sigma_{aa}^2}\right], & \text{if } \sigma_{aa} \gg \Gamma_a. \end{cases} \end{aligned} \quad (33)$$

One can see that this simple but generic description of light transmission through a loaded FPR fully complies with the considerations in Section 1. When the quality of the FPR mirrors is low [the upper case in Eq. (33)] the finite number of impurities inside the FPR cell leads only to a shift in the Lorentz resonant peaks $\langle V_{aa}\rangle = (1-1/\varepsilon)c$ because of a slight change in the mean dielectric constant. This simple result reveals an important way to measure the impurity concentration via a shift of resonant peaks in the FPR filled by impurities, as demonstrated in Fig. 3(c). In the regime of high-quality FPR mirrors $\Gamma_a \ll \sigma_a$, one can see from Eq. (33) that the Lorentz peaks are substituted with Gaussian resonant peaks. This is related to an inhomogeneous average of Lorentz peaks each shifted by V_{aa}.

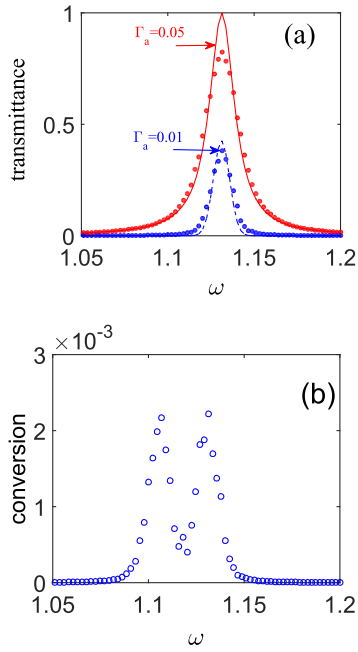

Fig. 4. (a) Average transmittance through the loaded FPR cell in the two-channel approximation. (b) Average channel conversion transmittance $\langle|T(p,q)^{(2)}|^2\rangle$. The parameters of the model are $\omega_a = 0.85, \omega_b = 1.15, \varepsilon = 1.25$, and $c = 0.25$.

The tendency of substitution of the Lorentz resonant peaks by the Gaussian peaks with a growth in the impurities concentration is seen in Figs. 3(a) and 3(b). The CMT approach in this section presented in Fig. 4(a) also clearly shows that. In addition to Fig. 3, we take the impurities concentration to be fixed but vary the quality of FPR mirrors Γ_a to demonstrate crossover from the clean regime to the regime of weak disorder.

In order to take into account the channel conversion, it is enough to keep in the CMT equations two eigenmodes $a = (m, p)$ and $b = (n, q)$ with eigenfrequencies close to the frequency of the injected wave. If there are no impurities, the eigenmodes are uncoupled. The perturbation Eq. (18) mixes the eigenmodes, giving rise to channel conversion. Derivation of the conversion amplitude $T^{(2)}(\omega)$ and average over the impurities is straightforward, however, rather cumbersome. In Fig. 4(b), we present a direct numerical solution of the CMT equations

$$\begin{aligned}\omega\psi_a &= (\omega_a + V_{aa} - i\Gamma_a)\psi_a + V_{ab}\psi_b - i\sqrt{\Gamma_a}E_0, \\ \omega\psi_b &= (\omega_b + V_{bb} - i\Gamma_b)\psi_b + V_{ab}\psi_a - i\sqrt{\Gamma_b}E_0, \end{aligned} \quad (34)$$

for channel conversion transmittance $\langle|T_{pq}^{(2)}(\omega)|^2\rangle$.

5. CONCLUDING REMARKS

The inclusion of dielectric particles with small cross sections results in Rayleigh scattering. Impurity particles placed in the Fabry–Perot resonator cause multiple scattering events which enhance Rayleigh scattering. Indeed, the numerical results show that the transmittance undergoes a noticeable

change with the growth of the impurity concentration from a slight shift of the Lorentz peak to a suppression of transmittance for high-quality FPR mirrors. The numerical approach is based on the discretized version of the effective non-Hermitian Hamiltonian which is equivalent to the coupled mode theory. We complemented the numerical results with analytical formulas for averaged transmittance, which show a transition from the regime of weak disorder for low-quality FPR mirrors to the regime of strong disorder described by Gaussian resonant peaks high-quality mirrors. For numerical simulations, we modeled dielectric impurity particles in the form of dielectric rods of squared cross section parallel to the FPR mirrors that reduce the dimension of the system to two. The approaches presented in the paper allow us to consider the three-dimensional case while accounting for both EM polarizations.

Funding. Russian Science Foundation (RSF) (14-12-00266).

Acknowledgment. This paper was a subject of numerous discussions with my colleagues E. N. Bulgakov, D. N. Maksimov, K. N. Pichugin, I. S. Sandalov, and V. Ya. Zyryanov, to whom I express my thanks. Also, the paper has enormously benefited from the input of six referees.

REFERENCES

1. Lord Rayleigh, "On the propagation of waves through a stratified medium, with special reference to the question of reflection," Proc. R. Soc. London Ser. A **86**, 207–226 (1912).
2. M. Lax, "Multiple scattering of waves," Rev. Mod. Phys. **23**, 287–310 (1951).
3. M. C. W. van Rossum and T. M. Nieuwenhuizen, "Multiple scattering of classical waves: microscopy, mesoscopy, and diffusion," Rev. Mod. Phys. **71**, 313–371 (1999).
4. A. Ishimaru, *Wave Propagation and Scattering in Random Media* (Academic, 1978).
5. C. Jin, R. Nadakuditi, E. Michielssen, and S. C. Rand, "Iterative, backscatter-analysis algorithms for increasing transmission and focusing light through highly scattering random media," J. Opt. Soc. Am. A **30**, 1592–1601 (2013).
6. V. V. Varadan and V. K. Varadan, "Multiple scattering of electromagnetic waves by randomly distributed and oriented dielectric scatters," Phys. Rev. D **21**, 388–394 (1980).
7. V. P. Tishkovets and K. Jockers, "Multiple scattering of light by densely packed random media of spherical particles: dense media vector radiative transfer equation," J. Quant. Spectrosc. Radiat. Transfer **101**, 54–72 (2006).
8. L. Margerin, "Mean-field T-matrix approach to elastic wave scattering by small and point-like objects," Waves Random Complex Media **21**, 628–644 (2011).
9. Z. Cui, Y. Han, and Q. Xu, "Numerical simulation of multiple scattering by random discrete particles illuminated by Gaussian beams," J. Opt. Soc. Am. A **28**, 2200–2208 (2011).
10. J. B. Pendry, A. MacKinnon, and A. B. Pretre, "Maximal fluctuations—a new phenomenon in disordered systems," Physica A **168**, 400–407 (1990).
11. O. N. Dorokhov, "Electron localization in a multichannel conductor," Sov. Phys. J. Exp. Theor. Phys. **58**, 606–615 (1983).
12. P. Exner, P. Gawlista, P. Šeba, and M. Tater, "Point interactions in a strip," Ann. Phys. **252**, 133–179 (1996).
13. R. Gebarowski, P. Šeba, K. Życzkowski, and J. Zakrzewski, "Quantum scattering in the strip: from ballistic to localized regimes," Eur. Phys. J. B **6**, 399–429 (1998).
14. E. N. Bulgakov, A. F. Sadreev, V. P. Gerasimov, and V. Y. Zyryanov, "Resonant angular conversion in Fabry–Perot resonator holding a dielectric cylinder," J. Opt. Soc. Am. A **31**, 264–267 (2014).
15. M. Born and E. Wolf, *Principles of Optics: Electromagnetic Theory of Propagation, Interference and Diffraction of Light* (Cambridge University, 1999).
16. P. Markos and C. M. Soukoulis, *Wave Propagation, From Electrons to Photonic Crystals and Left-Handed Materials* (Princeton University 2008), Chap. 10.
17. H. Feshbach, "Unified theory of nuclear reactions," Ann. Phys. **5**, 357–390 (1958).
18. H. Feshbach, "A unified theory of nuclear reactions. II," Ann. Phys. **19**, 287–313 (1962).
19. C. Mahaux and H. A. Weidenmüller, *Shell Model Approach in Nuclear Reactions* (Wiley, 1969).
20. I. Rotter, "A continuum shell model for the open quantum mechanical nuclear system," Rep. Prog. Phys. **54**, 635–682 (1991).
21. F. Dittes, "The decay of quantum systems with a small number of open channels," Phys. Rep. **339**, 215–316 (2000).
22. A. F. Sadreev and I. Rotter, "S-matrix theory for transmission through billiards in tight-binding approach," J. Phys. A **36**, 11413–11433 (2003).
23. E. N. Bulgakov and A. F. Sadreev, "Bound states in the continuum in photonic waveguides inspired by defects," Phys. Rev. B **78**, 075105 (2008).
24. D. N. Maksimov, A. F. Sadreev, A. A. Lyapina, and A. S. Pilipchuk, "Coupled mode theory for acoustic resonators," Wave Motion **56**, 52–66 (2015).
25. K. Pichugin, H. Schanz, and P. Seba, "Effective coupling for open billiards," Phys. Rev. E **64**, 056227 (2001).
26. A. I. Rahachou and I. V. Zozoulenko, "Light propagation in finite and infinite photonic crystals: the recursive Green's function technique," Phys. Rev. B **72**, 155117 (2005).
27. L. Martin, G. Di Giuseppe, A. Perez-Leija, R. Keil, F. Dreisow, M. Heinrich, S. Nolte, A. Szameit, A. F. Abouraddy, D. N. Christodoulides, and B. E. A. Saleh, "Anderson localization in optical waveguide arrays with off-diagonal coupling disorder," Opt. Express **19**, 13636–13646 (2011).
28. S. Datta, *Electronic Transport in Mesoscopic Systems* (Cambridge University, 1995).
29. I. Rotter and A. F. Sadreev, "Influence of branch points in the complex plane on the transmission through double quantum dots," Phys. Rev. E **69**, 066201 (2004).
30. A. Mitra, H. Harutyunyan, S. Palomba, and L. Novotny, "Tuning the cavity modes of a Fabry–Perot resonator using gold nanoparticles," Opt. Lett. **35**, 953–955 (2010).
31. S. Fan, W. Suh, and J. D. Joannopoulos, "Temporal coupled-mode theory for the Fano resonance in optical resonators," J. Opt. Soc. Am. A **20**, 569–572 (2003).
32. W. Suh, Z. Wang, and S. Fan, "Temporal coupled-mode theory and the presence of non-orthogonal modes in lossless multimode cavities," IEEE J. Quantum Electron. **40**, 1511–1518 (2004).